

PARAMETER ANALYSIS OF COPPER-NICKEL-TUNGSTEN PREPARED VIA
POWDER METALLURGY PROCESS FOR ELECTRICAL DISCHARGE
MACHINING OF POLYCRYSTALLINE DIAMOND

AINAA MARDHIAH BINTI SABRI

A thesis submitted in fulfilment of the
requirement for the award of the Degree of Master of
Mechanical Engineering

Faculty of Mechanical and Manufacturing Engineering
Universiti Tun Hussein Onn Malaysia

SEPTEMBER 2019

DEDICATION

SPECIAL GRATITUDE TO:

**Special for my parent,
SABRI BIN OMAR & MASIHAH BINTI MD. ZAIN
“Thanks for your continuous morale and support”
“Your inspiration will always with me”**

**Especially for my kind supervisor that give encouragement and support
DR. MOHAMMAD ZULAFIF BIN RAHIM
“Thanks for the knowledge and advice given”**

**My lovely siblings,
“Thanks for your support and encouragement in everything”**

Also, to all my friends that give full support,

**Only Allah S.W.T can repay your kindly
Hope Allah S.W.T blesses our life**

ACKNOWLEDGEMENT

Praise be to Allah, The Most Merciful, The Most Compassionate, for granting me the chance and strength to complete this thesis for Master Degree, which undoubtedly bring me into heights of intellectual and emotional enrichment.

My highest gratitude goes to my supervisor, Dr Mohammad Zulafif bin Rahim who throughout completing this research not only provides me with guidance, advice but generously also shares with me his insights and understanding needed to complete this project. Thus, I wish to express my deepest gratitude and appreciation to him for his generosity, critics and intellectual support. I also want to thank Associate Professor Ts. Dr. Mohd Rasidi Bin Ibrahim who assign as my co-supervisor and the lecturers and staffs of FKMP for their cooperation during the completion of the master research that had given valuable information, suggestions and guidance in the compilation and preparation master report.

Besides that, I would like to thank to all technicians and Precision Machining Research Centre (PREMACH) members who were willingly lending their helping hand in laboratory and experiment work. I extend my thankfulness to all my fellow friends. My deepest appreciation goes to my beloved family who always showers me in each and every moment with love, motivation and prayers.

I would like to acknowledge the Ministry of Higher Education (MOHE) Malaysia under Fundamental Research Grant Scheme (FRGS) grant, Vot 1586 (Parameter Correlation and Mechanism in Catalytic Erosion of Polycrystalline Diamond) for financial support.

Lastly, thanks a lot to those who had giving a hand, directly or indirectly in helping me to finish my research and thesis successfully.

ABSTRACT

Polycrystalline Diamond (PCD) tools have an outstanding wear resistance. The electric conductivity of PCD caused by the conductive binding material (Cobalt) makes it possible to machine PCD tools with EDM. Electrode used in EDM of PCD must have better porosity, electrical and thermal conductivity. Therefore, this research presents the works in production of Cu-Ni-W electrode by powder metallurgy route. Production of powder metallurgy parts involve mixing of the powder with additives or lubricants, compacting the mixture and heating the green compacts in an Argon gas furnace so the particle bond to each other. Two levels of full factorial with six centre points and two replication technique was used to study the influence of main and interaction effects of the powder metallurgy parameter. There were four factors involved in this experiment. Factor A which is Type of Cu-Ni; Type A and Type B was defined as categorical factor. Factor B in which Composition of W; 5 Wt.%, 15 Wt. % and 25 Wt.%, was defined as numerical factor. Factor C which is the Compaction load; 7, 8 and 9 tonne and Factor D which is Sintering temperature; 635 °C, 685 °C and 735 °C were also defined as numerical factor. Optical Microscope, Scanning Electron Microscopy (SEM) and Energy Dispersive X-ray (EDX) was used to analysed the microstructure and surface morphology of Cu-Ni-W electrode. The best parameter combination to produced better porosity, electrical and thermal conductivity for both Type A and Type B was 5 Wt.% of W, compaction load at 9 tonne and sintering temperature at 735°C. The best response for Type A is 12.65% of porosity, 14.40 IACS% of electrical conductivity and 413.26 W/m.°C of thermal conductivity. While that, the best response for Type B were 9.36% of porosity, 16.66 IACS% of electrical conductivity and 345.21W/m.°C of thermal conductivity. From the calculation of Maxwell's Equation, Type A and Type B had the highest electrical conductivity of 58.48 IACS% and 77.35 IACS% respectively at W content of 5Wt.%. Type A and Type B also had the highest thermal conductivity of 369.86 W/m.°C and 310.24 W/m.°C respectively at W content of 5 Wt.%. Besides that, thermal conductivity also increased with the temperature increased until 450°C.

ABSTRAK

Alat *Polycrystalline Diamond* (PCD) mempunyai rintangan haus yang bagus. Pemesinan EDM terhadap PCD dapat dilakukan disebabkan oleh bahan pengikat di dalam PCD iaitu kobalt mempunyai kekonduksian elektrik. Elektrod yang digunakan dalam pemesinan EDM terhadap PCD harus mempunyai keliangan yang lebih baik, kekonduksian elektrik dan haba. Oleh sebab itu, penyelidikan ini membentangkan produksi elektrod Cu-Ni-W dengan menggunakan kaedah metalurgi serbuk. Proses metalurgi serbuk melibatkan pencampuran serbuk dengan aditif atau pelincir, memampatkan campuran dalam acuan yang sesuai dan sampel dilakukan *sintering* dalam gas Argon. Dua tahap faktorial penuh dengan enam titik pusat dan dua teknik replikasi digunakan untuk mengkaji pengaruh kesan utama dan interaksi parameter metalurgi serbuk. Terdapat empat faktor yang terlibat dalam eksperimen ini. Faktor A ialah Jenis Cu-Ni; Jenis A dan Jenis B didefinisikan sebagai faktor berkategori. Faktor B di mana komposisi W; 5 Wt.%, 15 Wt.% dan 25 Wt.%, ditakrifkan sebagai faktor berangka. Faktor C iaitu Beban Pemasatan; 7, 8 dan 9 tan dan Faktor D ialah suhu Pembakaran; 635 °C, 685 °C dan 735 °C juga ditakrifkan sebagai faktor berangka. Mikroskop optik, Mikroskopi Pengimbasan Elektron (SEM) dan *Energy X-ray Dispersive* (EDX) digunakan untuk menganalisis struktur mikro dan permukaan morfologi Cu-Ni-W komposit. Gabungan parameter yang terbaik untuk menghasilkan keliangan yang lebih baik, kekonduksian elektrik dan haba untuk kedua-dua Jenis A dan Jenis B ialah dengan 5 Wt.% W, beban pepadatan pada 9 tan dan suhu sintering pada 735 °C. Tindakbalas best untuk Jenis A adalah 12.65% keliangan, 14.40 IACS% daripada kekonduksian elektrik dan 413.26 W / m. °C kekonduksian haba. Sementara itu, tindak balas best untuk Jenis B adalah 9.36% keliangan, 16.66 IACS% daripada kekonduksian elektrik dan 345.21 W / m. °C kekonduksian haba. Dari pengiraan dengan menggunakan persamaan *Maxwell*, Jenis A dan Jenis B didapati mempunyai kekonduksian elektrik yang tinggi iaitu 58.48 IACS% dan 77.35 IACS% setiap satu pada 5 Wt.% komposisi W. Pada 5 Wt.% komposisi W juga, kekonduksian haba maksimum bagi Jenis A adalah 369.86 W/m.°C dan Jenis B adalah 310.24 W/m.°C. Selain itu, dengan kenaikan suhu sehingga 450 °C, kekonduksian haba juga semakin meningkat.

CONTENTS

TITLE	i
DECLARATION	ii
DEDICATION	iii
ACKNOWLEDGEMENT	iv
ABSTRACT	v
ABSTRAK	vi
CONTENTS	vii
LIST OF TABLES	xi
LIST OF FIGURE	xiv
LIST OF SYMBOLS AND ABBREVIATION	xx
LIST OF APPENDICES	xxi
CHAPTER 1 INTRODUCTION	1
1.1 Background of Study	1
1.2 Problem Statement	4
1.3 Objectives of Study	4
1.4 Scope of Study	5
1.5 Significance of Study	5
CHAPTER 2 LITERATURE REVIEW	6
2.1 EDM Electrode	6
2.2 Important Properties of Electrode	7
2.2.1 Porosity Density	9
2.2.2 Thermal Conductivity	9

2.2.3	Electrical Conductivity	10
2.2.4	Material for Electrodes	11
2.3	Manufacturing of Electrode	12
2.3.1	Rapid Prototyping and Rapid Tooling	13
2.3.2	Casting Method	15
2.3.3	Powder Metallurgy	15
2.4	Influences of Process Parameter of Powder Metallurgy	18
2.4.1	Compaction Pressure	18
2.4.2	Sintering Temperature	19
2.5	Powder for Fabrication of Electrode via Powder Metallurgy Process	21
2.5.1	Copper powder	21
2.5.2	Nickel Powder	22
2.5.3	Tungsten Powder	22
2.6	Design of Experiment (DOE)	22
2.6.1	Level Full Factorial Experiment	23
2.6.2	Optimization in 2 Level Full Factorial Design	24
2.7	Previous Study On Powder Metallurgy Parameter	27
2.7.1	Effects of Powder Metallurgy Parameters on Porosity, Electrical Conductivity, Thermal Conductivity, and Microstructure	27
2.7.2	Summary of Previous Study of Cu-Ni-W composites	37
CHAPTER 3 METHODOLOGY		39
3.1	Introduction	39
3.2	Research Flow Chart	39

3.3	Material Selection	42
3.3.1	Copper Powder	42
3.3.2	Nickel Powder	43
3.3.3	Tungsten Powder	44
3.3.4	Binding Agent	45
3.4	Design of Experiment	46
3.4.1	2-level full factorial design	46
3.5	Fabrication of Copper-Nickel-Tungsten Composites	46
3.5.1	Sample Preparation	49
3.5.2	Mixing Process	49
3.5.3	Compaction Process	50
3.5.4	Sintering Process	51
3.6	Characterization of Sample Electrode	54
3.6.1	Porosity Density	54
3.6.2	Thermal Conductivity Test	55
3.6.3	Electrical Conductivity Test	57
3.6.4	Microstructure and Surface Morphology	58
CHAPTER 4 RESULT AND ANALYSIS		59
4.1	Preliminary Test	59
4.2	DOE Analysis	61
4.2.1	DOE Analysis of Porosity	62
4.2.2	DOE Analysis of Electrical Conductivity	78
4.2.3	DOE Analysis of Thermal Conductivity	95
4.2.4	Mathematical Model	109
4.2.5	Optimization Condition	111
4.2.6	Confirmation Test	118

4.3	Microstructure and Surface Morphology Analysis	120
4.4	Theoretical Value and Experimental Value for Electrical Conductivity	134
4.5	Theoretical Value and Experimental Value for Thermal Conductivity	136
4.6	The Effect of Temperature Dependence Properties of Thermal Conductivity	139
CHAPTER 5 CONCLUSION AND RECOMMENDATION		141
5.1	Introduction	141
5.2	Conclusion	141
5.3	Recommendation	143
REFERENCES		144
APPENDIX A		154
APPENDIX B		157
APPENDIX C		159



PTFA UTHM
PERPUSTAKAAN TUNKU TUN AMINAH

LIST OF TABLES

2.1	Layout of experimental for 2^4 full factorial design	24
2.2	Chemical Composition of the W-Cu composites [70]	32
2.3	Thermal Conductivity for W-Cu38 composites [70]	32
2.4	Summary of the reported research of Cu-Ni-W composites	38
3.1	Physical and Chemical Properties of Cu	42
3.2	Physical and Chemical Properties of Ni	43
3.3	Physical and Chemical Properties of W	44
3.4	Physical and Chemical Properties of Zinc Stearate	45
3.5	Factor and level for experiment	47
3.6	Full factorial design of experiment (sort by number of run)	47
3.7	Variation of Cu-Ni-W composites	49
4.1	Composition of Cu-Ni-W (preliminary)	60
4.2	Experimental Result of Porosity, electrical conductivity and thermal conductivity	61
4.3	Initial ANOVA (considering all factors) (porosity)	63
4.4	Revised ANOVA (porosity)	65
4.5	Summary of R-Squared value for Porosity Test	65
4.6	Initial ANOVA (considering all factors) (Electrical Conductivity)	80
4.7	Revised ANOVA (Electrical Conductivity)	81
4.8	Summary of R-Squared value for Electrical Conductivity Test	82
4.9	Initial ANOVA (considering all factors) (Thermal Conductivity)	96
4.10	Revised ANOVA (Thermal Conductivity)	97

4.11	Summary of R-Squared value for Thermal Conductivity Test	98
4.12	Best parameter combination to minimize Porosity (%) for Type A	112
4.13	Best parameter combination to minimize Porosity (%) for Type B	113
4.14	Best parameter combination to maximise Electrical Conductivity for Type A	114
4.15	Best parameter combination to maximise Electrical Conductivity for Type B	114
4.16	Best parameter combination to maximise thermal conductivity for Type A	115
4.17	Best parameter combination to maximise thermal conductivity for Type B	116
4.18	Best parameter combination to minimize Porosity (%) and maximise Electrical and Thermal Conductivity for Type A	117
4.19	Best parameter combination to minimize Porosity (%) and maximise Electrical and Thermal Conductivity for Type B	117
4.20	Parameter used for confirmation runs	118
4.21	Experimental result for confirmation runs (test number 1)	118
4.22	Experimental result for confirmation runs (test number 2)	119
4.23	Experimental result for confirmation runs (test number 3)	119
4.24	Experimental result for confirmation runs (test number 4)	119
4.25	Experimental result for confirmation runs (test number 5)	119
4.26	Experimental result for confirmation runs (test number 6)	120

4.27	Sample with lowest porosity (%), highest Electrical Conductivity and Highest Thermal Conductivity	131
4.28	EDX element of Cu-Ni-W composites at best parameter combination for Type A	132
4.29	EDX element of Cu-Ni-W composites at best parameter combination for Type B	133
4.30	Theoretical Value for Electrical Conductivity	134
4.31	Theoretical Value for Thermal Conductivity	136



LIST OF FIGURES

1.1	EDM illustration	2
2.1	Properties of good electrodes	8
2.2	Powder metallurgy process [48]	16
2.3	Powder Metallurgy Process [47]	16
2.4	Sintering cycle [52]	20
2.5	Distribution patterns of W powders and pores formed by W powders (a) distribution pattern of tetrahedron and (b) small W particles in the pore [56]	21
2.6	Flowchart representing the 2-level full factorial method for optimization [68]	26
2.7	SEM images of sintered composites with various Cu contents; (a) W-10 Wt.% Cu, (b) W-20 Wt.% Cu and (c) W-30 Wt.% Cu [71]	28
2.8	Microstructures of W-Cu composites, where: (a) W-20 Wt.% Cu and (b) W-30 Wt.% Cu [47]	29
2.9	Ni-rich phase as grey phase in sintered tungsten with 0.5 Wt.% Ni, sintering temperature of: 9a) 1450 °C and (b) 1550 °C [57]	30
2.10	Density of tungsten specimens after activated sintering vs. nickel amount [57]	30
2.11	Coefficient of thermal expansion CTE versus temperature for W-Cu composites compacted under 1200 MPa and sintered at 1400 °C for 2 h [49]	31
2.12	Electrical Conductivity of sintered composites with different sintering temperature [51]	33
2.13	SEM image of composited sintered at (a) 850°C and (b) 1050°C [51]	33

2.14	SEM image of the sample sintered at 850°C [54]	34
2.15	Thermal Conductivity of W-(Ni)-Cu composites against W content [10]	35
2.16	SEM morphology of W-70 Wt.% Cu composite powder [10]	35
2.17	Microstructures of W-(Ni)-Cu composites, (a)(b) W-Cu40Wt.%; (c)(d) W-Cu30Wt.%; (e)(f) W-Cu25Wt.%; (g)(h) W-Ni5Wt.%-Cu15Wt.%.[10]	36
2.18	Electrical and Thermal Conductivity [53]	37
3.1	Methodology Chart	41
3.2	Copper Powder, 45µm	42
3.3	Nickel Powder	43
3.4	Tungsten Powder	44
3.5	Zinc Stearate	45
3.6	Ball Milling Machine	49
3.7	Carver Hydraulic Press Machine	50
3.8	Size of Sample	51
3.9	Tube Furnace	52
3.10	Sintering cycle for Cu-Ni-W at 635°C	52
3.11	Sintering cycle for Cu-Ni-W at 685°C	53
3.12	Sintering cycle for Cu-Ni-W at 735°C	53
3.13	Metler Toledo XS64 Density meter	55
3.14	Schematic drawing for Thermal Conductivity Test	56
3.15	Pro4 for Electrical Conductivity Test	57
3.16	(a) Optical Microscope and (b) Scanning Electron Microscopy (SEM)	58
4.1	Half-Normal Plot Graph (considering all investigated factors)	62
4.2	Half normal plot graph for Porosity analysis	64
4.3	The normal plot of residual graph of Porosity	66
4.4	The residuals vs. predicted graph of Porosity	66
4.5	Perturbation Plot BCD for (a)Type A (90:10) and (b) B (70:30) towards Porosity	67

4.6	Effect of Main Factor A Type towards Porosity (%)	68
4.7	Effect of Main Factor B Composition towards Porosity (%) for (a) Type A and (b) Type B	69
4.8	Effect of Main Factor C Compaction Load towards Porosity (%) for (a) Type A and (b) Type B	70
4.9	Effect of Main Factor D Sintering Temperature towards Porosity (%) for (a) Type A and (b) Type B	71
4.10	Effect of Interaction Factor AB	72
4.11	Effect of Interaction Factor AC	73
4.12	Effect of Interaction Factor BC for Type A	74
4.13	Effect of Interaction Factor BC for Type B	75
4.14	Effect of Interaction Factor BD for Type A	76
4.15	Effect of Interaction Factor BD for Type B	76
4.16	Effect of Interaction Factor CD for Type A	78
4.17	Effect of Interaction Factor CD for Type B	78
4.18	Half-Normal Plot Graph (considering all investigated factors)	79
4.19	Half normal plot graph for Electrical Conductivity analysis	80
4.20	The normal plot of residual graph of Electrical Conductivity	83
4.21	Residual vs Predicted graph for Electrical Conductivity	83
4.22	Perturbation Plot BCD for Type A (90:10) and Type B (70:30) towards Electrical Conductivity	84
4.23	Effect of Main Factor A Type towards Electrical Conductivity	85
4.24	Effect of Main Factor B: Composition towards Electrical Conductivity for (a) Type A and (b) Type B	86
4.25	Effect of Main Factor C: Compaction Load towards Electrical Conductivity for (a) Type A and (b) Type B	87

4.26	Effect of Main Factor D: Sintering temperature towards Electrical Conductivity for (a) Type A and (b) Type B	89
4.27	Effect of Interaction Factor AB	90
4.28	Effect of Interaction Factor AC	91
4.29	Effect of Interaction Factor AD	91
4.30	Effect of Interaction Factor BD for Type A	92
4.31	Effect of Interaction Factor BD for Type B	93
4.32	Effect of Interaction Factor CD for Type A	94
4.33	Effect of Interaction Factor CD for Type B	94
4.34	Half-Normal Plot Graph (considering all investigated factors)	95
4.35	Half normal plot graph for Thermal Conductivity analysis	97
4.36	The normal plot of residual graph of Thermal Conductivity	98
4.37	Residual vs Predicted graph for Thermal Conductivity	99
4.38	Perturbation Plot BCD for Type A (90:10) and Type B (70:30) towards Thermal Conductivity	100
4.39	Effect of Main Factor A Type towards Thermal Conductivity	101
4.40	Effect of Main Factor B: Composition towards Thermal Conductivity for (a) Type A and (b) Type B	102
4.41	Effect of Main Factor C: Compaction Load towards Thermal Conductivity for (a) Type A and (b) Type B	103
4.42	Effect of Main Factor D: Sintering temperature towards Thermal Conductivity for (a) Type A (b) Type B	104
4.43	Effect of Interaction Factor AC	105
4.44	Effect of Interaction Factor BC for Type A	106
4.45	Effect of Interaction Factor BC for Type B	107
4.46	Effect of Interaction Factor BD for Type A	108

4.47	Effect of Interaction Factor BD for Type B	108
4.48	Optical microscopy image of Type A of Cu-Ni-W with 5 Wt.% of W, compacted at 7 tonne and sintered at (a) 635°C (b) 735°C	121
4.49	Optical microscopy image of Type A of Cu-Ni-W with 5 Wt.% of W, compacted at 9 tonne and sintered at (a) 635°C (b) 735°C	121
4.50	Optical microscopy image of Type A of Cu-Ni-W with 25 Wt.% of W, compacted at 7 tonne and sintered at (a) 635°C (b) 735°C	122
4.51	Optical microscopy image of Type A of Cu-Ni-W with 25 Wt.% of W, compacted at 9 tonne and sintered at (a) 635°C (b) 735°C	122
4.52	Optical microscopy image of Type B of Cu-Ni-W with 5 Wt.% of W, compacted at 7 tonne and sintered at (a) 635°C (b) 735°C	123
4.53	Optical microscopy image of Type B of Cu-Ni-W with 5 Wt.% of W, compacted at 9 tonne and sintered at (a) 635°C (b) 735°C	124
4.54	Optical microscopy image of Type B of Cu-Ni-W with 25 Wt.% of W, compacted at 7 tonne and sintered at (a) 635°C (b) 735°C	124
4.55	Optical microscopy image of Type B of Cu-Ni-W with 25 Wt.% of W, compacted at 9 tonne and sintered at (a) 635°C (b) 735°C	125
4.56	SEM image of Type A of Cu-Ni-W with 5 Wt.% of W, compacted at 7 tonne and sintered at (a) 635°C (b) 735°C	126
4.57	SEM image of Type A of Cu-Ni-W with 5 Wt.% of W, compacted at 9 tonne and sintered at (a) 635°C (b) 735°C	126

4.58	SEM image of Type A of Cu-Ni-W with 25 Wt.% of W, compacted at 7 tonne and sintered at (a) 635°C (b) 735°C	127
4.59	SEM image of Type A of Cu-Ni-W with 25 Wt.% of W, compacted at 9 tonne and sintered at (a) 635°C (b) 735°C	127
4.60	SEM image of Type B of Cu-Ni-W with 5 Wt.% of W, compacted at 7 tonne and sintered at (a) 635°C (b) 735°C	128
4.61	SEM image of Type B of Cu-Ni-W with 5 Wt.% of W, compacted at 9 tonne and sintered at (a) 635°C (b) 735°C	129
4.62	SEM image of Type B of Cu-Ni-W with 25 Wt.% of W, compacted at 7 tonne and sintered at (a) 635°C (b) 735°C	130
4.63	SEM image of Type B of Cu-Ni-W with 25 Wt.% of W, compacted at 9 tonne and sintered at (a) 635°C (b) 735°C	130
4.64	Graph of Electrical Conductivity versus Composition of W of Theoretical value and experimental value at sintering temperature 735°C for Type A and B	136
4.65	Graph of Thermal Conductivity versus Composition of W	138
4.66	Graph of Thermal Conductivity versus Temperature for Type A and Type B	140

LIST OF SYMBOLS AND ABBREVIATION

Cu	-	Copper
Cu-Ni	-	Copper-nickel
Cu-Ni-W	-	Copper-nickel-tungsten
EDM	-	Electrical Discharge Machining
PCD	-	Polycrystalline Diamond
Ni	-	Nickel
W	-	Tungsten
O	-	Oxygen
C	-	Carbon
W	-	Watts
°C	-	Degree Celsius
M	-	Meter
K	-	Kelvin
μ	-	Micro
Λ	-	Thermal Conductivity
Σ	-	Electrical Conductivity
P	-	Density
G	-	gram
Cm ³	-	Centimetre cubic
Wt. %	-	Weight Percentage
Rpm	-	Revolution per minutes
SEM	-	Scanning Electron Microscopy
EDS	-	Energy Dispersive X-ray Spectroscopy
IACS%	-	International Annealed Copper Standard

LIST OF APPENDICES

APPENDIX	TITLE	PAGE
A	Apparatus to Calculate Q for Thermal Conductivity	152
B	List of Publications	155
C	Material Safety Data Sheet	157



CHAPTER 1

INTRODUCTION

1.1 Background of Study

Diamond is among the hardest material in the world that is produced through sintering process of selected diamond particles at high temperature and high-pressure condition. Due to the outstanding wear resistance of Polycrystalline Diamond (PCD) manufactured by sintering selected diamond particles, cutting tools made of PCD have extensive tool life and outstanding performance in machining non-ferrous metals and non-metallic materials [1]. However, PCD tools are very difficult to fabricate and the high manufacturing costs of PCD tools seriously impede its application in the industry. Since 2010, extensive research has been initiated to increase PCD machining efficiency and tool quality [2, 3]. However, there is no substantial development has been achieved due to the lack of innovative approaches and new theories to solve the two fundamental problems in machining PCD; the ultra-hardness of diamond particles and the low electrical conductivity of PCD material. This leads to the high manufacturing cost caused by the long machining time that becomes a major drawback to the application of PCD tools: a brazed PCD tool is about 10 times expensive than a W carbide tool, and the price of a vined PCD tool is about 20 times higher than the carbide ones [4].

Electrical Discharge Machining (EDM) is a noncontact thermal erosion process in which the metal is removed by a series of recurring electrical discharges between the electrode and the electrically conductive work piece, in the presence of dielectric fluid. Figure 1.1 shows the illustration of the basic components of the EDM process. The electric conductivity of PCD caused by the conductive binding material (Cobalt) makes it possible to machine PCD tools with EDM. However, the low electrical conductivity of Polycrystalline Diamond makes the EDM process almost

three times slower than EDM of conductive metals. The crucial problem that causes low machining efficiency in EDM of PCD is the low electricity conductivity of PCD [5].

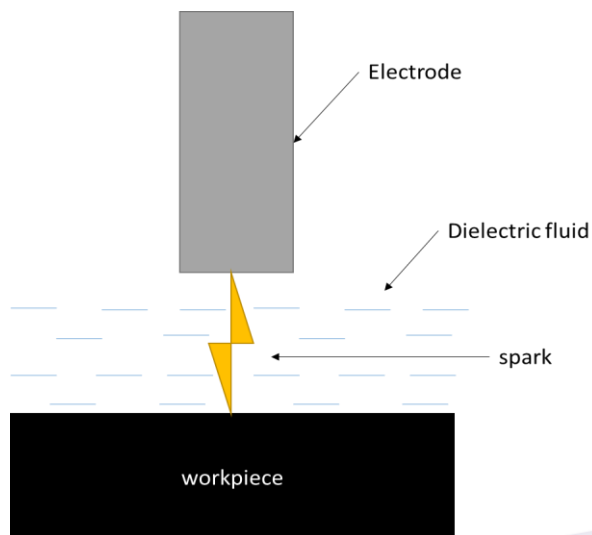


Figure 1.1: EDM illustration

Electrode used in Electrical Discharge Machining plays an important role to improve the efficiency of machining that is considered as a tool in EDM process. Electrode acts as a path for electrical current to be supplied to the sparking position. The acceleration of electrode towards the workpiece will generate heat and cause erosion. The performance of EDM process is largely dependent on electrode material and manufacturing process. The electrode that is able to provide the highest material removal rate (MRR) and the lowest tool wear is the most desired [6]. In this case, the electrode material properties such as electrical conductivity, thermal conductivity, and melting point should be considered in addition to the manufacturability and cost [7].

Copper (Cu) electrode is normally used for Electrical Discharge Machining of ordinary material due to its high electrical and thermal conductivity. The electrode is mentioned to offer fine surface finish of product without the requirement of secondary process of polishing [7]. To improve the wear resistant of the electrodes, Tungsten (W) that has high melting point is normally added [8]. Since slow erosion process in PCD EDM causes a significant electrode wear ratio, this improvised Cu electrode (named as Copper Tungsten, Cu-W) plays an important role in this application. Though

recently, it was mentioned that the Cu-Ni electrode provides better surface finish than Cu-W electrode in micro-EDM of PCD [9].

As short circuit pulse frequently appears during the PCD EDM process (PCD is touching the electrode), there is a high probability of graphitisation catalyst process taking place. When diamond particles come into contact with the graphitisation catalyst material (in this case Nickel (Ni)) at high temperature, carbon atoms in diamond will be diffused. Hence, it is possible for the graphitization of diamond particles to be accelerated (catalyst phenomenon). Thus, melting temperature of PCD surface reduces significantly due to the acceleration of graphitization (diamond to graphite conversion) that consequently increases the MRR.

In this research, the development of Copper-Nickel Tungsten (Cu-Ni-W) electrode properties is believed to provide better improvement in Electrical Discharge Machining of Polycrystalline Diamond. It is different from the manufacturing of Cu-W electrode where very small composition of Ni is usually added as activator during solid phase sintering in powder metallurgy route, in which higher content of Ni is purposely added [10]. The Ni not only acts as the activator during solid phase sintering, but also as the catalyst during Electrical Discharge Machining of Polycrystalline Diamond.

Manufacturing of EDM electrodes is usually done by using conventional alloying technique which is casting. However, this technique is found suitable only for less complex electrodes material composition [6]. In fact, significant differences in melting temperature of alloying materials give challenge to the casting process. In the case of Cu-Ni-W production, Cu with vaporisation temperature of 2595°C is expected to vaporize first before tungsten begins to melt at temperature 3422°C [11]. Hence, powder metallurgy is believed to provide better ability in combining several alloying materials. Due to this reason, powder metallurgy is selected as the manufacturing process to produce the Cu-Ni-W electrode in this research.

1.2 Problem Statement

Nowadays, there are a number of electrodes available in the market for Electrical Discharge Machine. These include Cu-Ni, Cu-W, Cu, brass, and graphite[12, 13, 14]. However, there is no electrode purposely developed for EDM of PCD. Market available Cu-Ni is able to provide better surface roughness of eroded PCD but believed as unable to deliver at least similar wear resistant as Cu-W electrode [9]. Moreover, until now, there is no Cu-Ni-W electrode available in the market, thus limits its exploration and application in PCD EDM [15, 16, 17]. The emergence of Cu-Ni-W electrode is expected to overcome the limitation. However, the information on the manufacturing process of this electrode is limited. In fact, the information on electrode development using powder compaction is only limited to a certain material only, such as Cu-W [18, 19]. Hence the information on thermal and electrical characteristic of the Copper-Nickel-Tungsten (Cu-Ni-W) electrode produced by the process is also limited [20, 21].

1.3 Objectives of Study

The aim of the project is to develop an electrode purposely designed for Electrical Discharge Machining of Polycrystalline Diamond.

The detailed objectives are:

- i) To determine the significant parameter that influences the porosity, electrical and thermal conductivity of Cu-Ni-W by using Design of Experiment (DOE) Analysis.
- ii) To investigate the effect of different powder metallurgy process parameter on porosity density, electrical and thermal conductivity of the Cu-Ni-W Composites.
- iii) To analyse the surface morphology and microstructure of Cu-Ni-W composites prepared with different process parameter.

REFERENCES

1. Hsu F. C., Tai T. Y., Vo V. N., Chen S. Y., and Chen Y. H. The machining characteristics of polycrystalline diamond (PCD) by micro-WEDM. *Procedia CIRP*. 2013. 6: 261–266.
2. Iwai M., Ninomiya S., and Suzuki K. Effect of Complex Electro discharge Grinding for Electrically Conductive PCD. *Advanced Materials Research*. 2011. 325: 276–281.
3. Qinjian Z., Luming Z., Jianyong L., Yonglin C., Heng W., Yunan C., Haikuo S., Xiaoqing Y., Minzhi L. Study on Electrical Discharge and Ultrasonic Assisted Mechanical Combined Machining of Polycrystalline Diamond. *Procedia CIRP*. 2013. 6, 589–593.
4. Modern Machine Shop (2008). Could The Highest Price Cutter Be The Least Expensive? An evaluation of different cutting tool technologies for machining carbon fiber reinforced plastics. Retrieved on May 27, 2018, from <https://www.mmsonline.com/articles/could-the-highest-price-cutter-be-the-least-expensive>
5. Rahim M.Z. Research on Electrical Discharge Machining of Polycrystalline. Ph.D. Thesis. RMIT University; 2015.
6. Patel N. Review on Importance of Electrodes in Electrical Discharge Machining Process. *International Journal of Research in Aeronautical and Mechanical Engineering*. 2015. 3(10): 36–41.
7. Kern R. Sinker Electrode Material Selection. *EDM Today*. July/August, 2008.
8. Hamidi A. G., Arabi H., and Rastegari S. A feasibility study of W-Cu composites production by high pressure compression of tungsten powder. *International Journal of Refractory Metals and Hard Materials*. 2011. 29(1): 123–127.

9. Haikal Ahmad, M. A. Zulafif Rahim, M. Mohd Fauzi, M. F. Hafizah Azis, N. Ismail, A. E. Fahrul Hassan, Mohd Arifin, A.M.T. Yusof, M. S., Rasidi Ibrahim, M. "Electrical Discharge Machining of Polycrystalline Diamond Using Copper Electrode - Finishing Condition. *IOP Conference Series: Materials Science and Engineering*. 2017. 203(1): 1-6.
10. Yan A., Wang Z., Yang T., Wang Y., Ma Z. Microstructure, thermal physical property and surface morphology of W-Cu composite fabricated via selective laser melting. *Materials and Design*. 2016. 109: 79–87.
11. Balkanski M. Springer Series in Chemical Physics 39: laser Processing and Diagnostics. Verlag Berlin Heidelberg. Springer, 1984.
12. Khan A. A. Electrode wear and material removal rate during EDM of aluminum and mild steel using copper and brass electrodes. *International Journal of Advanced Manufacturing Technology*. 2008. 39: 482–487.
13. Amorim F. L. and Weingaertner W. L. The behavior of graphite and copper electrodes on the finish die-sinking electrical discharge machining (EDM) of AISI P20 tool steel. *Journal of the Brazilian Society of Mechanical Sciences and Engineering*. 2008. 29(4): 366–371.
14. Amorim F.L., Schäfer G.; Stedile L.J., Bassani I.A. On the Behaviour of Parameters and Copper -Tungsten Electrode Edge Radius Wear When Finishing Sinking EDM of Tool. *IMW - Institutsmittteilung*. 2010. 35: 121-140.
15. Yan J., Watanabe K., and Aoyama T. Micro-electrical discharge machining of polycrystalline diamond using rotary cupronickel electrode. *CIRP Annals-Manufacturing Technology* .2014., vol. 63(1): 209–212.
16. Rahim M. Z., Li G., Ding S., Mo J., Brandt M. Electrical discharge grinding versus abrasive grinding in polycrystalline diamond machining-tool quality and performance analysis *International Journal of Advanced Manufacturing Technology*. 2016. 85(1-4): 263–277.
17. Rahim M. Z., Ding S., Mo J. Electrical Discharge Grinding of Polycrystalline Diamond- Effect of Machining Parameters and Finishing In-Feed. *Journal of Manufacturing Science and Engineering*. 2014. 137(2): 1-11.
18. Kim J., Ryu S., Kim Y. Do, and Moon I. Densification Behaviour On Mechanically Alloyed W-Cu Composite Powders by the Double Rearrangement Process. *Scripta Materialia*. 1998. 39(6): 669–676.

19. Gu D. and Shen Y. Effects of processing parameters on consolidation and microstructure of W-Cu components by DMLS. *Journal of Alloys and Compounds journal*. 2009. 473: 107–115.
20. Duan L., Lin W., Wang J., and Yang G. Thermal properties of W-Cu composites manufactured by copper infiltration into tungsten fibre matrix. *International Journal of Refractory Metals and Hard Materials*. 2014. 46: 96–100.
21. Wei K. X., Wei W., Wang F., Du Q. B., Alexandrov I. V., and Hu J. Microstructure, mechanical properties and electrical conductivity of industrial Cu-0.5%Cr alloy processed by severe plastic deformation. *Materials Science and Engineering A*. 2011. 528(3): 1478–1484.
22. Jameson, E.C. Description and development of electrical discharge machining (EDM). *Electrical Discharge Machining*. Dearborn. Michigan., Society of Manufacturing Engineers. pp.32; 2001.
23. Ho K. H., Newman S. T., Rahimifard S., and Allen R. D. State of the art in wire electrical discharge machining (WEDM). *International Journal of Machine Tools and Manufacture*. 2004. 43(13): 1247–1259.
24. Liu K., Lauwers B., and Reynaerts D. Process capabilities of Micro-EDM and its applications. *International Journal Advance Manufacturing Technology*. 2010. 47: 11–19.
25. Jha B., Ram K., and Rao M. An overview of technology and research in electrode design and manufacturing in sinking electrical discharge machining. *Journal of Engineering Science and Technology Review*. 2011. 4(2): 118–130.
26. Shrestha B. *Designing an Electrode for Electrical Discharge Machining (EDM)*. Bachelor's Degree Thesis. Arcada University of Applied Sciences. 2014.
27. Rajurkar K. P., Sundaram M. M., and Malshe A. P. Review of electrochemical and electrodischarge machining. *Procedia CIRP*. 2013. 6: 13–26.
28. Tsai H. C., Yan B. H., and. Huang F. Y. EDM performance of Cr/Cu-based composite electrodes. *International Journal Machine Tools and Manufacture*. 2003. 4(3): 3245–252.
29. Nor S. S. M., Rahman M. M., Tarlochan F., Shahida B., and Ariffin A. K. The effect of lubrication in reducing net friction in warm powder compaction process. *Journal of Materials Processing Technology*. 2008. 207: 118–124.

30. Dutta G. and Bose D. Effect of Sintering Temperature on Density, Porosity and Hardness of a Powder Metallurgy Component. *International Journal of Emerging Technology and Advanced Engineering*. 2012. 2(8): 121–123.
31. Agrawal A. and Satapathy A. Development of a heat conduction model and investigation on thermal conductivity enhancement of AlN/epoxy composites *Procedia Engineering*. 2013. 51: 73–578.
32. Ali Khan A., Ndaliman M. B., Md. Soot H., and Ishak N. Influence Of Thermal Conductivity Of Electrodes On EDM Process Parameters 1. *Australian Journal of Basic and Applied Sciences*. 2012. 6(9): 337-345.
33. EDM Machining (2000). *All About EDM Machining (Electrical Discharge Machining)*. EDM Machining Process & Techniques. Retrieved on April 10, 2018, from <http://www.edmmachining.com/>
34. Dan O., Dana M. L., and Vasile L. Effective electrical conductivity estimation for a novel multi-phase composite material. *Proceedings of the 8th WSEAS International Conference on Microelectronics, Nanoelectronics, Optoelectronics*. May 2009. Brasov Romania. Transilvania University. 2009. pp. 111–114.
35. Che Haron C. H., Ghani J. A, Burhanuddin Y., Seong Y. K., and Swee C. Y. Copper and graphite electrodes performance in electrical-discharge machining of XW42 tool steel. *Journal of Materials Processing Technology*. 2008. 201(1): 570–573.
36. Zaw H. M., Fuh J. Y. H., Nee A. Y. C., and Lu L. Formation of a new EDM electrode material using sintering techniques. *Journal of Materials Processing Technology*. 1999. 89–90:182–186.
37. Garg R. K., Singh K. K., Sachdeva A., Sharma V. S., Ojha K., and Singh S. Review of research work in sinking EDM and WEDM on metal matrix composite materials. *International Journal Advanced Manufacturing Technology*. 2010. 50(5–8): 611–624.
38. Mathalai Sundaram C., Sivasubramanian R., and Sivakumar M. Development of new metal matrix composite electrodes for electrical discharge machining through powder metallurgy process. *Carbon - Science and Technology*. 2014. 6(4): 34–40.

39. Sabri A.M., Rahim M.Z., Ahmad M.A.H, Azis N.H. The Effect of Powder Metallurgy Parameters on Electrical Conductivity of Copper-Nickel-Tungsten Electrode. *International Journal of Engineering Technology*. 2019.8(1.1): 111–116.
40. Rahmati S. Rapid Tooling Development. In: *Rapid Prototyping Technology – Principles and Functional Requirements*. Iran: Islamic Azad University (IAU). pp. 55-80; 2014.
41. Campbell R. I. and. Bernie M. R. N. Creating a database of rapid prototyping system capabilities. *Journal of Materials Processing Technology*. 1996. 61(1–2): 163–167.
42. Beaman J., Agarwala M., Barlow J., Marcus H., and Bourell D. Direct selective laser sintering of metals. *Rapid Prototyping Journal*. 2002. 1(1):26–36.
43. Arthur A., Dickens P.M, Cobb R.C. Using rapid prototyping to produce electrical discharge machining. *Rapid Prototyping Journal*. 2007. 2(1):4–12.
44. Zhao J., Li Y., Zhang J., Yu C., and Zhang Y. Analysis of the wear characteristics of an EDM electrode made by selective laser sintering. *Journal of Materials Processing Technology*. 2003.138(1–3): 475–478.
45. Samuel M. P.and Philip P. K. Power metallurgy tool electrodes for electrical discharge machining. *International Journal of Machine Tools and Manufacture*. 1997. 37(11):1625–1633.
46. Beri N., Maheshwari S., Sharma C., and Kumar A. Surface Quality Modification Using Powder Metallurgy Processed CuW Electrode During Electric Discharge Machining of Inconel 718. *Procedia Material Science*. 2014. 5: 2629–2634.
47. Ibrahim A., Abdallah M., Mostafa S. F., and Hegazy A. A. An experimental investigation on the W-Cu composites. *Materials Design*. 2009. 30(4): 1398–1403.
48. Beri N., Maheshwari S., Sharma C., and Kumar A. Technological Advancement in Electrical Discharge Machining with Powder Metallurgy Processed Electrodes: A Review. *Materials and Manufacturing Processes*. 2010. 25: 1186–1197.
49. Abu-Oqail A., Ghanim M., El-Sheikh M., and El-Nikhaily A. Effects of processing parameters of tungsten-copper composites. *International Journal of Refractory Metals and Hard Materials*. 2012. 35: 207–212.

50. Mahani Y. and Zuhailawati H. Effect of Compaction Pressure on Microstructure and Properties of Copper-Based Composite Prepared by Mechanical Alloying and Powder Metallurgy. *International Journal of Materials, Mechanics and Manufacturing*. 2013. 795:343–346.
51. Yusoff M. and Hussain Z. Effect of Sintering Parameters on Microstructure and Properties of Mechanically Alloyed Copper-Tungsten Carbide Composite. *International Journal of Materials, Mechanics and Manufacturing*. 2013. 1(3): 283–286.
52. Li L., Wong Y. S., Fuh J. Y. H, and Lu L. EDM performance of TiC/copper-based sintered electrodes. *Material Design*. 2002. 22(8): 669–678.
53. Li C., Zhou Y., Xie Y., Zhou D., and Zhang D. Effects of milling time and sintering temperature on structural evolution, densification behavior and properties of a W-20Wt.%Cu alloy. *Journal of Alloys and Compounds*. .2018. 731: 537–545.
54. Gowon B., Mohammed K. S., Baharin S., Jamaluddin B., Hussain Z., and Evarastics P. The Effects of Sintering Temperature on the Densification of Mechanically Alloyed W-Brass Composites. *Open Journal of Metal*. 2015.5:19–26.
55. Vettivel S. C., Selvakumar N., and Leema N. Experimental and prediction of sintered Cu-W composite by using artificial neural networks. *Material Design*. 2013. 45:323–335.
56. Bin Liu B., Xie J. X., and Qu X. H. Fabrication of W-Cu functionally graded materials with high density by particle size adjustment and solid-state hot press. *Composites Science and Technology*. 2008. 68(6): 1539–1547.
57. Hamidi A. G., Arabi H., and Rastegari S. Tungsten-copper composite production by activated sintering and infiltration. *International Journal of Refractory Metals and Hard Materials*. 2011. 29(4):538–541.
58. Moon I. H., Lee J. S., Moon I. H, and Lee J. S., “Activated Sintering of Tungsten-Copper Contact Materials,” *Powder Metallurgy*. 1979. 22(1): 5–7.
59. Well. H.G. Chapter 21-Design and Analysis of Experiments. In: *Data Science for Business and Decision Making*. Elsevier Inc. pp. 935–939; 2019.
60. Singh P. K., Patel D., and. Prasad S. B. Optimization of process parameters during Vibratory welding technique using Taguchi’s analysis. *Perspectives in Science*, 2016. 8: 399-402.

61. Kamaruddin S, Khan Z. A., and Foong S. H. Application of Taguchi Method in the Optimization of Injection Moulding Parameters for Manufacturing Products from Plastic Blend. *International Journal of Engineering and Technology*. 2010. 2(6): 574–580.
62. Almeida M., Erthal R., Padua E., Silveira L., and Am L. Talanta Response surface methodology (RSM) as a tool for optimization in analytical chemistry. *Talanta journal*. 2008. 76: 965–977.
63. Karkalos E. and Markopoulos A. P. Numerical investigation of heat-induced effects on steel workpieces during hard turning machining process. *Journal of Chemical Technology and Metallurgy*. 2017. 52(2): 288–293.
64. Altinkok N. Application of the full factorial design to modelling of Al₂O₃ / SiC particle reinforced al-matrix composites. *Steel and Composite Structure*. 2019. 21(6): 1327-1345.
65. Barka N., Abdennouri M., Boussaoud. A, Galadi A., Baalala M. Full factorial experimental design applied to oxalic acid photocatalytic degradation in TiO₂ aqueous suspension. *Arab Journal of Chemistry*. 2014. 7(5): 752–757.
66. Kumar L., Sreenivasa Reddy M., Managuli R. S., and Pai K. G. Full factorial design for optimization, development and validation of HPLC method to determine valsartan in nanoparticles. *Saudi Pharmaceutical Journal*. 2015. 23(5): 549–555.
67. Suresh Kumar G., Padmanabhan G. and Dattatreya Sarma B. Optimizing the temperature of hot outlet air of vortex tube using Taguchi method. *Procedia Engineering*. 2014. 97: 828–836.
68. R. T. Ogulata and S. M. Mezarcioz, “Optimization of air permeability of knitted fabrics with the Taguchi approach,” *J. Text. Inst.*, vol. 102, no. 5, pp. 395–404, 2011.
69. Raison M. and Mark F. Z. Application of two-level full factorial design and response surface methodology in the optimization of inductively coupled plasma-optical emission spectrometry (ICPOES) instrumental parameters for the determination of platinum,” *Journal of Geology and Mining Research*. 2017. 9(5): 43–53.
70. Khosla A., Kumar S., and Aggarwal K. K. K. Identification of strategy parameters for particle swarm optimizer through Taguchi method. *Journal of Zhejiang University Science A*. 2006. 7(12): 1989–1994.

71. Kim Y. D., Oh N. L., Oh S. T. and Moon I. H. Thermal conductivity of W-Cu composites at various temperatures. *Materials Letters*.2001. 51(5): 420-424
72. Lee S. H., Kwon S. Y., and Ham H. J. Thermal conductivity of tungsten-copper composites. *Thermochimica. Acta*. 2012. 542: 2-5.
73. Chen P., Luo G., Shen Q., Li M., and Zhang L. Thermal and electrical properties of W-Cu composite produced by activated sintering. *Materials and Design*. 2014. 46: 101-105.
74. Chauhan D., Singhvi N., and Singh R. Dependence of effective thermal conductivity of composite materials on the size of filler particles. *Journal of Reinforced Plastics and Composites*. 2013. 32(18): 1323-1330.
75. Pietrak K. and Winiewski T. S. A review of models for effective thermal conductivity of composite materials. *Journal of Power Technologies*. 2015. 95(1): 14-24.
76. Ibrahim H., Aziz A., and Rahmat A. Enhanced liquid-phase sintering of W-Cu composites by liquid infiltration. *International Journal of Refractory Metals and Hard Materials*. 2014. 42: 222-226.
77. Johnson J. L, Brezovsky J. J., and German R. M.Effects of tungsten particle size and copper content on densification of liquid-phase-sintered W-Cu. *Metallurgical and Materials Transactions A: Physical Metallurgy and Materials Science*. 2005. 36(10): 2807–2814.
78. Mondal A., Upadhyaya A., and Agrawal D. Effect of Heating Mode and Copper Content on the Densification of W-Cu Alloys. *Indian Journal of Materials Science*, 2013. 2013: 1–7.
79. Luo S., Yi J., Guo Y., Peng Y., Li L., Ran J. Microwave sintering W – Cu composites: Analyses of densification and microstructural homogenization. *Journal of Alloys and Compounds*.2009. 473: 5–9.
80. Celebi E. G., Yener T., Altinsoy I., Ipek M., Zeytin S., and Bindal C. The effect of sintering temperature on some properties of Cu-SiC composite. *Journal of Alloys and Compounds*. 2011. 509(20): 6036–6042.
81. Islak S. Kir, D., and Buytoz S. Effect of sintering temperature on electrical and microstructure properties of hot-pressed Cu-TiC composites. *Science of Sintering*. 2014. 46(1): 15-21.
82. Mackenzie J. K. and Shuttleworth R. A phenomenological theory of development. *Proceedings of the Physical Society*. 1949. 62(1): 833–852.

83. Slotwinski J. A., Garboczi E. J., and Hebenstreit K. M. Porosity Measurements and Analysis for Metal Additive Manufacturing Process Control. *Journal of Research of the National Institute of Standards and Technology*. 2014. 119: 494.
84. A. S. M. International, A. R. Reserved, A. S. M. R. Reference, M. Properties, and M. D. Book. Part 1. 2000.
85. Abbaszadeh H., Masoudi A., Safabinesh H., and Takestani M. Investigation on the characteristics of micro- and nano-structured W-15 Wt.%Cu composites prepared by powder metallurgy route. *International Journal of Refractory Metals and Hard Materials*. 2014. 30(1): 145–151.
86. Dong L. L., Ahangarkani M., Chen W. G., and Zhang Y. S. Recent progress in development of tungsten-copper composites: Fabrication, modification and applications. *International Journal of Refractory Metals and Hard Materials*, 2018. 75: 30–42.
87. Johnson J. L. Activated liquid phase sintering of W – Cu and Mo – Cu. *International Journal of Refractory Metals and Hard Materials*. 2015. 53: 80–86.
88. Jabur A. S. Effect of powder metallurgy conditions on the properties of porous bronze. *Powder Technology*. 2013. 437: 477–483.
89. Vincent C., Silvain J. F., Heintz J. M., and Chandra N. Effect of porosity on the thermal conductivity of copper processed by powder metallurgy. *Journal of Physics and Chemistry of Solids*. 2012. 73(3): 499–504.
90. Ardestani M. Compaction and solid-state sintering behavior of Cu-20Wt.% ZnO powders. *Kovove Material*. 2013. 51: 367-371.
91. Hiraoka Y., Inoue T., Hanado H., and Akiyoshi N. Ductile-to-Brittle Transition Characteristics in W-Cu Composites with Increase of Cu Content. *Materials Transactions*. 2005. 46(7): 1663–1670.
92. Yan W., Li N., Li Y., Liu G., Han B., and Xu J. Effect of particle size on microstructure and strength of porous spinel ceramics prepared by pore-forming in situ technique. *Bulletin of Materials Science*. 2011. 34(5): 1109–1112.
93. Upadhyaya G. S., Powder Metallurgy Technology. England: Cambridge International Science Publishing. 2002.
94. Selvakumar N. and. Vettivel S. C. Thermal, electrical and wear behavior of sintered Cu – W nanocomposite. *Materials and Design*. 2013. 46:16–25.

95. Kang H. Tungsten / copper composite plates prepared by a modified powder-in-tube method. *Scripta Materialia*. 2004. 51: 473–477.
96. Chu K., Jia C. C., Liang X. B., and Chen H. Effect of sintering temperature on the microstructure and thermal conductivity of Al/diamond composites prepared by spark plasma sintering. *International Journal of Minerals, Metallurgy and Materials*. 2010. 17(2): 234–240.
97. Amirjan M., Zangeneh-Madar K., and Parvin N. Evaluation of microstructure and contiguity of W/Cu composites prepared by coated tungsten powders. *International Journal of Refractory Metals and Hard Materials*. 2009. 27(4): 729–733.
98. Montealegre-meléndez I., Arévalo C., Perez-soriano E. M., Neubauer E., Rubio-escudero C., and Kitzmantel M. Analysis of the Influence of Starting Materials and Processing Conditions on the Properties of W / Cu Alloys. *Materials (Basel)*. 2017. 10: 42.
99. Xu L., Srinivasakannan C., Zhang L., Yan M., Peng J., Xia H. and Guo S. Fabrication of tungsten-copper alloys by microwave hot pressing sintering. *Journal of Alloys and Compounds*, 2015.
100. Gonen M., Balkose D., Fikret I., and Semra U. Zinc Stearate Production by Precipitation and Fusion Processes. *Industrial & Engineering Chemistry Research*. 2005. 90: 1627–1633.
101. Singh. K and Kumar D. To Study the Effect of Copper Tungsten and Cryogenic Copper Tungsten Electrode on Material Removal Rate During Electrical Discharge Machining of H11. *International Journal of Mechanical Engineering and Robotic Research*. 2015. 4(1): 224-233.